Dual oxidase enables insect gut symbiosis by mediating respiratory network formation

Seonghan Jang[a,b], Peter Mergaert[c,1], Tsubasa Ohbayashi[c,d], Kota Ishigami[a], Shuji Shigenobu[e], Hideomi Itoh[b], and Yoshitomo Kikuchi[a,b,1]

[a]Graduate School of Agriculture, Hokkaido University, 060-8589 Sapporo, Japan; [b]Bioproduction Research Institute, National Institute of Advanced Industrial Science and Technology (AIST), 062-8517 Sapporo, Japan; [c]Université Paris-Saclay, CEA, CNRS, Institute for Integrative Biology of the Cell (I2BC), 91198 Gif-sur-Yvette, France; [d]Institute for Agro-Environmental Sciences, National Agriculture and Food Research Organization (NARO), 305-8604 Tsukuba, Japan; and [e]NIBB Core Research Facilities, National Institute for Basic Biology, 444-8585 Okazaki, Japan

Edited by Nancy A. Moran, The University of Texas at Austin, Austin, TX, and approved January 26, 2021 (received for review October 18, 2020)

Most animals harbor a gut microbiota that consists of potentially pathogenic, commensal, and mutualistic microorganisms. Dual oxidase (Duox) is a well described enzyme involved in gut mucosal immunity by the production of reactive oxygen species (ROS) that antagonizes pathogenic bacteria and maintains gut homeostasis in insects. However, despite its nonspecific harmful activity on microorganisms, little is known about the role of Duox in the maintenance of mutualistic gut symbionts. Here we show that, in the bean bug *Riptortus pedestris*, Duox-dependent ROS did not directly contribute to epithelial immunity in the midgut in response to its mutualistic gut symbiont, *Burkholderia insecticola*. Instead, we found that the expression of Duox is tracheae-specific and its down-regulation by RNAi results in the loss of dityrosine cross-links in the tracheal protein matrix and a collapse of the respiratory system. We further demonstrated that the establishment of symbiosis is a strong oxygen sink triggering the formation of an extensive network of tracheae enveloping the midgut symbiotic organ as well as other organs, and that tracheal breakdown by Duox RNAi provokes a disruption of the gut symbiosis. Down-regulation of the hypoxia-responsive transcription factor Sima or the regulators of tracheae formation Trachealess and Branchless produces similar phenotypes. Thus, in addition to known roles in immunity and in the formation of dityrosine networks in diverse extracellular matrices, Duox is also a crucial enzyme for tracheal integrity, which is crucial to sustain mutualistic symbionts and gut homeostasis. We expect that this is a conserved function in insects.

symbiosis | Duox | *Burkholderia* | *Riptortus pedestris* | trachea

Many animals possess a gut microbiota that is composed of pathogenic, commensal, and mutualistic microorganisms (1, 2). In insects, gut symbiotic microorganisms play a broad range of physiological roles in host metabolism and immunity through digestion of food, supplementation of essential nutrients that are scarce in food, degradation of phytotoxins and pesticides, and prevention of pathogen invasion by stimulation of the host immune system, production of antibiotics, or competition for limited nutrients and colonization sites (1, 3–6). Keeping symbiotic populations in the gut poses specific challenges: the hosts should specifically sustain the beneficial microbes while, at the same time and place, they need to winnow out pathogens and parasites acquired through feeding. To maintain gut homeostasis, some insects have evolved a symbiont sorting organ or filter in the gut (7, 8) or develop a specific gut compartment called the crop or crypt to harbor beneficial microbes (9). Specific physiological conditions in the gut lumen, such as pH, osmotic pressure, and oxygen concentration probably also contribute to create the favorable conditions for gut symbiosis. Except for gut symbionts in wood-feeding insects and honeybees, most insects' gut symbionts are aerobic bacteria belonging to the Proteobacteria (10, 11), suggesting that oxygen supplementation is critical to maintain quality and quantity of the gut symbiont population. However, it is poorly understood how the oxygen supply to the gut is established and how it affects the gut symbiosis.

In addition, studies in *Drosophila* have revealed that gut mucosal immunity plays an important role to eliminate unfavorable bacteria and to keep gut homeostasis (12, 13). Ingested bacteria, especially pathogens that come in contact with the gut epithelia, activate immune responses such as the production of antimicrobial peptides (AMPs) and reactive oxygen species (ROS) (14, 15). The activated gut immunity maintains the gut homeostasis by eliminating the invading environmental microbes, which may be harmful to the host. In particular, bactericidal ROS produced by the membrane-bound enzyme dual oxidase (Duox) is thought to antagonize bacterial growth and play a major role in gut mucosal immunity (12, 13, 16–20). Duox generates ROS via its C-terminal NADPH oxidase domain that produces H_2O_2 in the gut lumen and its N-terminal peroxidase-homology domain that converts the H_2O_2 into highly bactericidal hypochlorous acid. In *Drosophila* fed with a gut pathogen, silencing of *Duox* led to an increased pathogen load in the gut and the death of the insect (12). It was proposed that the Duox- and ROS-dependent immunity in the gut is dominant over AMP production that serves as a failsafe system in case of infection with ROS-resistant microbes (21).

Significance

The insect respiratory system consists of tubular tracheae that transport oxygen to the organs. We show that, in the insect pest *Riptortus pedestris*, the establishment of an essential symbiosis in the gut with the aerobic bacterial species *Burkholderia insecticola* triggers the development of an extensive tracheal network enveloping the gut. Genetically blocking the trachea formation prevents this gut symbiosis. We further discovered that the reactive oxygen species-generating enzyme Duox is crucial for the formation and stabilization of tracheae by forming protein cross-links in the tracheal matrix. Reactive oxygen species generated by Duox can be scavenged with antioxidants such as N-acetylcysteine, and feeding insects with this compound prevents tracheal formation and symbiosis, suggesting that antioxidants can be used as novel insecticides.

Author contributions: S.J., P.M., and Y.K. designed research; S.J., T.O., K.I., and H.I. performed research; S.J., P.M., S.S., H.I., and Y.K. analyzed data; and S.J., P.M., and Y.K. wrote the paper.

The authors declare no competing interest.

This article is a PNAS Direct Submission.

[1]To whom correspondence may be addressed. Email: peter.mergaert@i2bc.paris-saclay.fr or y-kikuchi@aist.go.jp.

This article contains supporting information online at https://www.pnas.org/lookup/suppl/doi:10.1073/pnas.2020922118/-/DCSupplemental.

Published March 1, 2021.

In addition to the direct immune function, Duox-mediated ROS also contributes to gut homeostasis in insects by stabilizing the peritrophic membrane of the midgut through the formation of covalent dityrosine bonds between matrix proteins (22, 23). The peritrophic matrix of insects forms a layer composed of chitin and glycoproteins that lines the midgut lumen. This layer protects the midgut epithelium from abrasive food particles and microbes. In the mosquito *Anopheles gambiae*, *Duox*-RNA interference (RNAi) leads to the disruption of a dityrosine network (DTN), which cross-links proteins in the peritrophic membrane, and a loss of the matrix's barrier function (23). Consequently, gut microbes gain direct contact with gut epithelial cells and activate chronic AMP expression, which provokes in turn a dramatic reduction of the bacterial midgut population. A similar function of Duox was reported in the tick *Ixodes scapularis* (24). Thus, Duox can interact in the insect gut with ingested microbes in two ways, by producing bactericidal ROS or by generating a physical barrier. In contrast to these well-described functions in mucosal immunity, little is known about the impact of the Duox enzyme on mutualistic bacteria.

The bean bug *Riptortus pedestris* (Fig. 1*A*), a notorious pest of legume crops, has a particular symbiotic organ located in the posterior midgut (25–27) (Fig. 1*B*). This region, called M4, is composed of several hundred crypts organized in two parallel rows. The lumen of these crypts is entirely filled with a specific gut symbiont of the genus *Burkholderia*. This is a nutritional symbiosis based on recycling by the gut symbiont of insect metabolic waste into high-value metabolites used by the host (28). This interaction is essential for optimal development and reproduction of the bean bug host (26). Every new generation of *R. pedestris* acquires the symbiont from the environmental soil by oral intake during feeding and drinking. A narrow channel located in the midgut, at the entrance of the M4, as well as microbe–microbe competition in the gut crypts, sorts out the specific partner from the ingested soil microbiota, resulting in the specific colonization of the symbiotic organ (7, 29). The few hundreds of bacterial cells that are taken up by the symbiotic organ during infection multiply in a few days to a population of tens of millions that completely occupy the luminal space of all the crypts in the M4 (30). The crypts control this very large symbiont population using immune-related AMPs as well as M4-specific symbiotic peptides (28, 31–33).

Given the cardinal role of ROS produced by Duox in insect gut immunity and the fact that the *Burkholderia* symbionts stay in direct contact with the crypt epithelial cells (34), we postulated in this study that, besides the AMPs, Duox and ROS are also involved in the management of the symbiosis in the midgut crypts of *R. pedestris*. However, our findings did not support an antimicrobial immune function of Duox, but revealed an unanticipated pivotal role for the enzyme in the formation of a tracheal network enveloping the symbiotic organ, which is in turn essential for supplying sufficient oxygen for respiration to the symbiotic organ and the aerobic gut symbiont.

Results

Gut Symbionts Induce the Generation of *R. pedestris* Duox-Dependent ROS in the *R. pedestris* Midgut. To determine if the gut symbiont *Burkholderia insecticola* induces ROS in the symbiotic organ of *R. pedestris*, we measured the relative ROS level in the lysate of dissected gut compartments of apo-symbiotic and symbiotic insects (Apo and Sym insects, respectively) using the fluorescent dye 2′,7′-dichlorofluorescein diacetate. An approximately threefold higher level of ROS was detected in the symbiotic organ of Sym insects compared to that of Apo insects, confirming that the colonization of the crypts by the *B. insecticola* symbiont stimulates ROS production (Fig. 1*C*). Moreover, the ROS level in the digestive tract of the midgut, the M1, M2, and M3 anterior regions (Fig. 1*B*), equally increased after symbiont colonization, indicating that the colonization by *B. insecticola* induces systemic high ROS levels throughout the whole midgut regions even if the symbiont resides only in the posterior symbiotic midgut region M4 (Fig. 1 *B* and *C*). To demonstrate whether Duox generates the symbiont-mediated ROS, the homologous gene of *R. pedestris* (*RpDuox*) was down-regulated by RNAi (*SI Appendix*, Fig. S1*A*). The *RpDuox* transcript was identified based on homology with the *Drosophila melanogaster* protein in a *R. pedestris* transcriptome dataset generated from the infected symbiotic organ. We found one *RpDuox* copy in *R. pedestris*, displaying 74.7% homology, and the encoded protein had all the functional domains of typical Duox proteins from insects to humans (22) (Fig. 1*D*). *RpDuox*-RNAi reduced the ROS level in the symbiotic organ, as well as in the other midgut regions of Sym insects, to a similar level as Apo insects (Fig. 1*C*), demonstrating that induction of ROS by symbiont colonization is due to Duox activity. Similarly, the feeding of Sym insects with the antioxidant compound *N*-acetylcysteine (NAC) (35), added to the drinking water, also decreased the ROS levels of the midgut regions to similar concentrations as in Apo insects (Fig. 1*C*). Taken together, these results demonstrate that the infection of *B. insecticola* induces production of ROS in the entire midgut region via the RpDuox enzyme.

RpDuox-Produced ROS Is Important for the Gut Symbiosis but Not as a Microbicidal Molecule. The production of infection-associated ROS is compatible with a mucosal immune response directed against the gut symbiont in the symbiotic organ. To test this hypothesis, we estimated the population size of symbionts in the M4 of Sym, *RpDuox*-RNAi ($Sym^{RpDuox\text{-}RNAi}$), and NAC-fed ($Sym^{NAC\text{-}fed}$) insects by qPCR. In *Drosophila*, silencing of *Duox* led to a reduced microbicidal ROS production and a concomitant increased total number of gut microbes (12). However, contrary to *Drosophila*, the titer of the *Burkholderia* symbiont in the M4 of *R. pedestris* was decreased more than 100 times in *RpDuox*-RNAi insects compared to Sym insects (Fig. 1*E*). Also, feeding of the antioxidant NAC to Sym insects reduced the number of gut symbionts to similarly low levels (Fig. 1*E*). Microscopy analysis confirmed that *RpDuox*-RNAi and NAC feeding caused the collapse of the symbiosis (Fig. 1*F*). Laser scanning microscopy and transmission electron microscopy (TEM) images showed that, in the symbiotic organ of *RpDuox*-RNAi and NAC-fed insects, gut symbionts were present close to the epithelial surface of the midgut crypts, but few symbionts were observed in the interior part of the crypt lumen (Fig. 1*F*). These results indicate that RpDuox plays a pivotal role in controlling gut symbiosis, but by a mechanism that is unrelated to a bactericidal action of ROS against the symbiont.

We next investigated the possible relation of RpDuox activity and bacterial infection and multiplication in the anterior digestive regions of the midgut. Although the ROS level was significantly decreased in M3 by *RpDuox*-RNAi (Fig. 1*C*), we found that the survival rate of *R. pedestris* after oral infection with the entomopathogen *Serratia marcescens* was not affected (Fig. 2*A*), suggesting that removing Duox-mediated ROS production did not render the insects more susceptible to the pathogen. Accordingly, the number of *S. marcescens* cells in the M3 region of the midgut was not significantly changed after *RpDuox* RNAi (Fig. 2*B*). Moreover, the number of *B. insecticola* cells that were transiently present in the M3 region after symbiont ingestion was also not altered in *RpDuox*-RNAi insects (Fig. 2*C*). Together, these results demonstrate that Duox-mediated ROS generation is not important to regulate the bacterial titer of pathogens or symbionts in the nonsymbiotic midgut regions.

Immune Stimulation by *RpDuox*-RNAi Is Not Responsible for Symbiosis Collapse. In addition to its bactericidal activity, Duox-mediated ROS is also known to contribute to the construction of the midgut peritrophic membrane, as shown in *A. gambiae* (23). Knockdown of

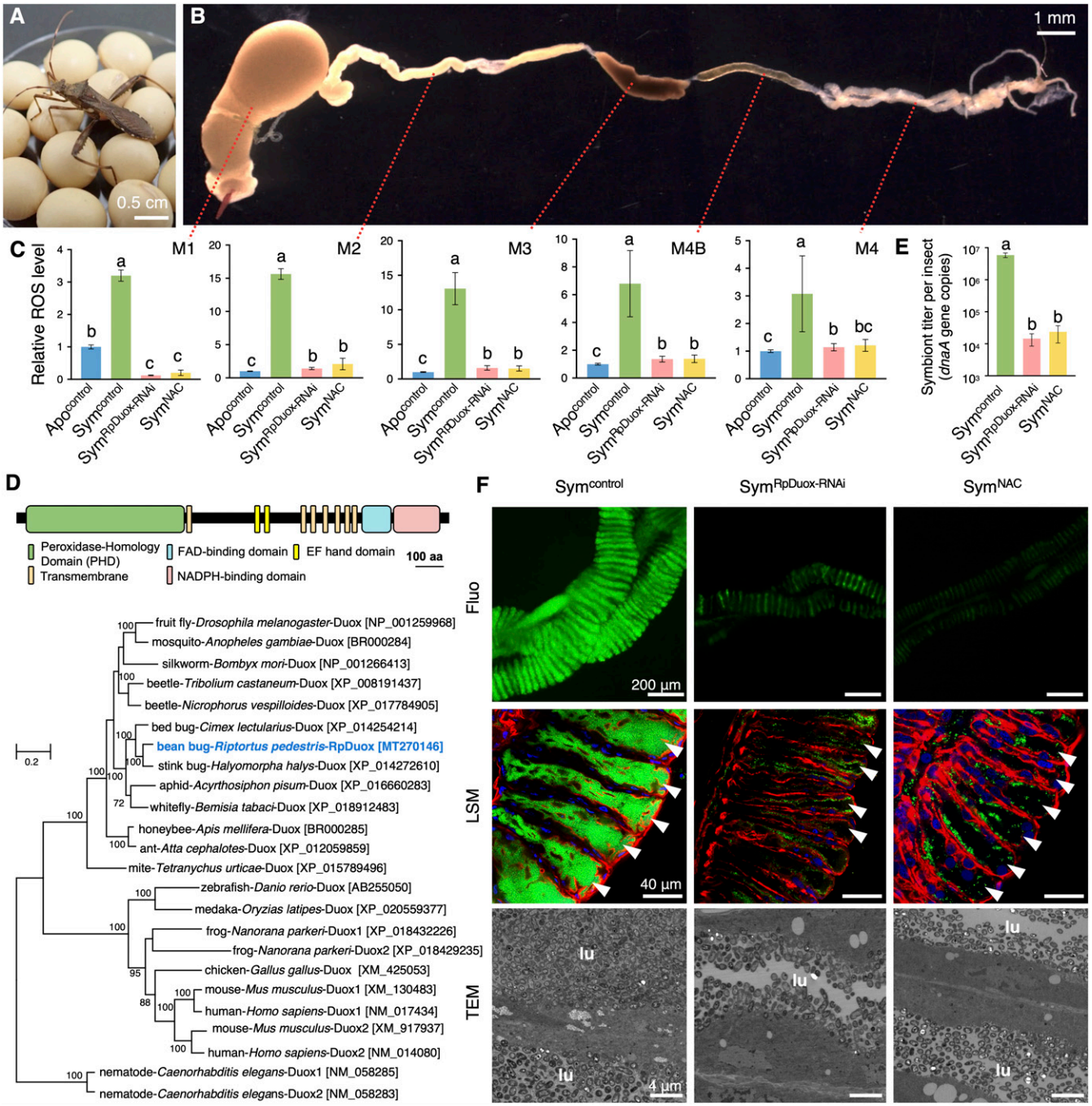

Fig. 1. RpDuox-mediated ROS is important for gut symbiosis. (*A*) An adult male *R. pedestris* feeding on soybeans. (*B*) The dissected midgut of *R. pedestris.* (*C*) Relative ROS level in the different midgut regions of Apo (Apo^{control}), Sym (Sym^{control}), *RpDuox*-RNAi (Sym$^{RpDuox\text{-}RNAi}$), and NAC-fed (Sym^{NAC}) insects. All values were normalized by the ROS level of Apo insects. (*D*) The predicted domains of the RpDuox protein (*Top*). Maximum-likelihood phylogeny based on amino acid sequences (*Bottom*). Numbers in parentheses indicate accession numbers. Bootstrap values (>60%) are shown near each node. (*E*) The number of symbionts colonizing the M4. Data shown in *C* and *E* are mean ± SD of $n = 9$ and $n = 6$ insects, respectively. Different letters indicate statistically significant differences ($P < 0.05$). The statistical significance of differences between samples was analyzed by a Kruskal–Wallis test with Bonferroni correction. (*F*) Microscopy images of the M4: epifluorescence microscopy (first row), laser scanning confocal microscopy (second row; green, symbionts; blue, host nuclei; red, host cytoskeleton; white arrowheads, midgut crypts), and transmission electron microscopy (third row; lu, luminal region of the midgut crypt).

duox in *A. gambiae* leads to a decreased barrier function of the peritrophic matrix and enhanced immune stimulation and AMP expression by gut microbes coming in close contact with epithelial cells. However, in contrast with the majority of insects, most hemipteran insects, including *R. pedestris*, do not possess a peritrophic membrane in the midgut (36). Nevertheless, the gene-expression profile comparison between the symbiotic organs of Sym and *RpDuox*-RNAi insects showed that expression of immunity-related genes, especially genes encoding AMPs (37), was increased in the midgut of *RpDuox*-RNAi insects (Fig. 2 *D* and *E*), but not in the fat body (Fig. 2*F*). It should be noted, however, that this up-regulated AMP gene expression in the midgut by *RpDuox*-RNAi was

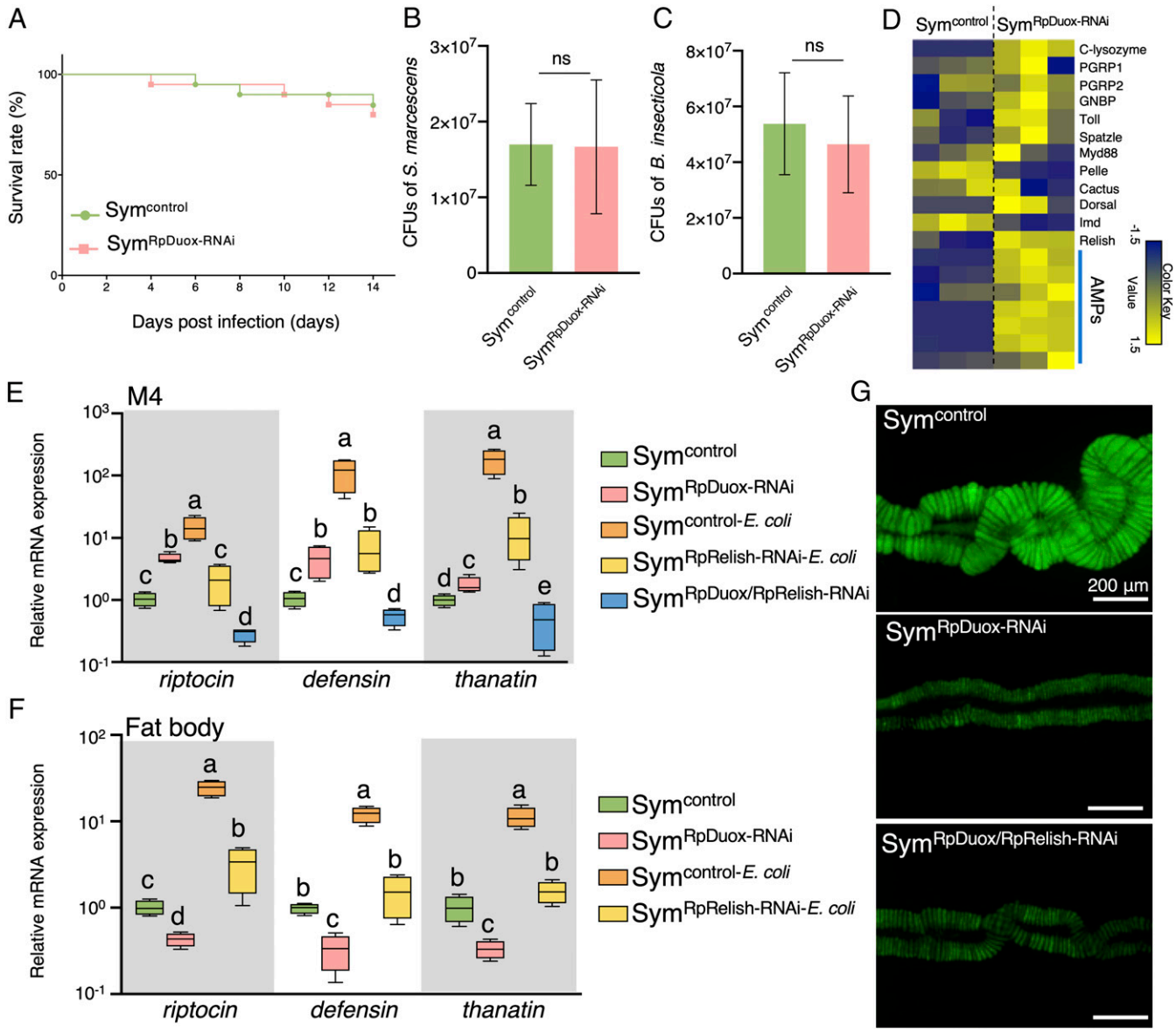

Fig. 2. RpDuox function is not related to gut mucosal immunity in the bean bug. (*A*) The survival rate of Sym (Sym^{control}) and *RpDuox*-RNAi (Sym$^{RpDuox\text{-}RNAi}$) insects after oral infection with 10^7 cells per milliliter of *S. marcescens* ($n = 20$ insects). (*B*) Number of *S. marcescens* colonies from the M3 region of third-instar nymph Sym^{control} and Sym$^{RpDuox\text{-}RNAi}$ insects. (*C*) The number of *Burkholderia* symbionts in the M3 of the third-instar nymph Sym^{control} and Sym$^{RpDuox\text{-}RNAi}$ insects. CFU, colony-forming units. (*D*) Expression profile from RNA sequencing data of immunity-related genes in the M4 of Sym^{control} and Sym$^{RpDuox\text{-}RNAi}$ insects. Each column is a replicate experiment. (*E*) The expression level of AMPs in the M4 of Sym insects without immune stimulation (Sym^{control}), Sym^{control} with septic injury by *Escherichia coli* injection in the hemolymph (Sym$^{control\text{-}E.\ coli}$), *RpRelish*-RNAi with *E. coli* injection (Sym$^{RpRelish\text{-}RNAi\text{-}E.coli}$), *RpDuox*-RNAi without bacterial injection (Sym$^{RpDuox\text{-}RNAi}$), and double *RpDuox*/*RpRelish*-RNAi insects without bacterial injection (Sym$^{RpDuox/RpRelish\text{-}RNAi}$). (*F*) The expression level of AMPs in the fat body. Data shown in *B* and *C* are from $n = 5$ insects, and those in *E* and *F* are from $n = 4$ insects. Different letters indicate statistically significant differences ($P < 0.05$). The statistical significance was analyzed by the Mann–Whitney *U* test (*B* and *C*) or Kruskal–Wallis test with Bonferroni correction (*E* and *F*). Error bars indicate SDs; ns, not statistically significant. (*G*) Effect of *RpDuox*/*RpRelish* double RNAi on symbiosis. Green color indicates the GFP signal from gut-colonizing *Burkholderia* symbionts.

significantly lower than in immune-stimulated insects by septic injury (Fig. 2 *E* and *F*). Because induced immunity in the symbiotic organ could antagonize the gut symbiont and thus, in principle, be at the origin of the symbiosis defect in *RpDuox*-RNAi insects, we aimed at knocking down the expression of the AMP genes in the bean bug. In the brown-winged green bug *Plautia stali*, a stinkbug related to *R. pedestris* in the infraorder Pentatomomorpha but belonging to a different family, the NF-κB transcription factor Relish of the Imd pathway is an essential regulator of AMP gene expression (38). *RpRelish*-RNAi in *R. pedestris* reduced the expression of all three tested AMP genes in the symbiotic organ as well as the fat body, indicating that, also in *R. pedestris*, Relish is a critical regulator of the expression of the AMP immune effectors (Fig. 2 *E* and *F*). After simultaneously silencing both *RpRelish* and *RpDuox*, the AMP expression was not up-regulated anymore in the symbiotic organ (Fig. 2*E*), showing that the induced AMP expression in the M4 by knockdown of *RpDuox* is dependent on the canonical Imd immune pathway. Importantly, the green fluorescent protein (GFP) signal of *Burkholderia* gut symbionts in double *RpDuox*/*RpRelish*-RNAi insects was not restored to control levels but remained similar to

single *RpDuox*-RNAi insects (Fig. 2*G* and *SI Appendix*, Fig. S2). Therefore, we can conclude that the up-regulation of the immune response does not directly contribute to disrupting the symbiotic relationship in *RpDuox*-RNAi insects.

Symbiont Colonization Triggers Tracheal Development, and RpDuox-Mediated ROS Stabilizes the Respiratory Network by Forming a Dityrosine Network. Thus, contrary to our initial expectation, the role of RpDuox and the ROS produced by it in the *R. pedestris–Burkholderia* symbiosis is not related to mucosal gut immunity. To find a clue leading to the specific function of *RpDuox* in the symbiosis, we measured its tissue-specific expression by RT-qPCR. Surprisingly, the expression of the *RpDuox* gene in Apo and Sym insects was incomparably high in the tracheae relative to all other tested tissues, suggesting that the RpDuox-mediated generation of ROS may have an important function in the respiratory system for maintaining gut symbiosis (Fig. 3*A*). Although the expression level of *RpDuox* in Sym insects was slightly higher than in Apo insects, the gene was also very strongly expressed in the tracheae of the latter insects, indicating that *RpDuox* is constitutively expressed in the tracheal network (Fig. 3*A*). The insect tracheal system consists of a tubular epithelial network containing a luminal chitin and protein matrix (23, 39–41). High *RpDuox* expression levels in the tracheae could be in agreement with the previously documented function of Duox-mediated ROS in shaping extracellular matrices by forming dityrosine cross-links between proteins and thereby creating a DTN (22). Immunostaining of a dissected midgut by a dityrosine-specific antibody indeed revealed the presence of a DTN enveloping the symbiotic organ of *R. pedestris* that likely corresponds to a respiratory network composed of tracheae and tracheoles (Fig. 3*B*). In addition to protein, chitin is another major constituent of the tracheal matrix (41). Chitin staining with calcofluor-white Fluorescent Brightener 28 revealed a tracheal network around the symbiotic organ that colocalized with the network revealed with the dityrosine-specific antibody (Fig. 3*C*), confirming that the DTN highlights tracheae and that dityrosines are abundant in them. Interestingly, both chitin and dityrosine staining revealed that the tracheal network enveloping the symbiotic organ and the tracheoles connecting inside the midgut crypt tissue developed much stronger in Sym insects compared to Apo insects (Fig. 3*D*). This morphological response suggests that colonization of the crypts by the large number of the *Burkholderia* gut symbiont is an oxygen-requiring process that induces the development of the respiratory network to supply enough oxygen to the symbiotic organ. Moreover, the tracheal network, especially the ramified tracheoles, did develop in response to the colonization of the gut symbiont *Burkholderia*, not only around the crypt-bearing M4 but also in the other midgut regions as well as the fat body (*SI Appendix*, Fig. S3 *A* and *B*), indicating that the activity of the symbiotic organ provokes a systemic oxygen stress in the whole insect body. This is furthermore in agreement with the ROS accumulation in all midgut regions (Fig. 1*C*). Accordingly, the higher ROS levels in the midgut of Sym insects compared to Apo insects resulted from the strongly developed attached tracheal network, since their careful removal from the symbiotic organ significantly reduced the detected ROS level (*SI Appendix*, Fig. S1*B*). Strikingly, the DTN as well as the chitin mesh in the symbiotic organ of Sym insects was strongly reduced by *RpDuox*-RNAi or feeding with the antioxidant NAC (Fig. 3*D*). Thus, RpDuox is indispensable for the establishment of the symbiosis-induced tracheal network in *R. pedestris*, and the increased ROS level in the midgut produced by RpDuox after symbiont infection is associated with the development of a tracheal network along the different midgut regions. The RNAi inactivation of *RpDuox* also abolished the formation of the enhanced tracheal network in the digestive, anterior midgut regions M1, M2, and M3 (*SI Appendix*, Fig. S3*A*) as well as the fat body (*SI Appendix*, Fig. S3*B*). These observations are in agreement with the suppression of *RpDuox* expression in the entire insect body, as can be expected from the double-stranded RNA (dsRNA) injection procedure to induce gene silencing.

Destabilization of the Respiratory Network by *RpDuox*-RNAi Causes Hypoxia in the Midgut. Based on these findings, we made the hypothesis that the collapse of the respiratory system by *RpDuox*-RNAi will cause a hypoxic environment in the symbiotic organ. We first measured in the crypt epithelial cells the activity of the mitochondria using MitoTracker dye. In Sym insects, a high number of active mitochondria was detected in the epithelial cells of the crypts of the symbiotic organ, which was drastically decreased after *RpDuox*-RNAi (Fig. 4*A*). Correspondingly, the expression of genes encoding the mitochondrial respiratory chain was down-regulated in *RpDuox*-RNAi insects (Fig. 4*B*), confirming that the symbiotic organ entered into a hypoxic condition after *RpDuox*-RNAi. Moreover, staining the symbiotic organ with Image-IT dye, which is a real-time hypoxia indicator, revealed a high fluorescence in the epithelia of the midgut crypts after *RpDuox*-RNAi compared with control Sym insects, further supporting that the disorganization of the respiratory network by *RpDuox* silencing causes hypoxia of the symbiotic organ (Fig. 4*A*). Of note, our finding that AMP-encoding genes are up-regulated in the hypoxic M4 of *RpDuox*-RNAi insects in a Relish-dependent manner (Fig. 2 *D* and *E*) mirrors previous findings in *Drosophila*, demonstrating that a hypoxic environment activates the expression of AMPs via the Toll and IMD pathways (42, 43).

Hypoxia could reduce the metabolic activity (43) of the crypt epithelial cells and their capacity to feed the bacterial symbiont, thereby provoking the collapse of the symbiosis. Some insect genes related to glycolysis and most genes of the tricarboxylic acid cycle were down-regulated in the M4 after *RpDuox*-RNAi, indicating that the metabolic activity of the crypt epithelial cells was indeed lower in *RpDuox*-RNAi insects than in Sym insects (*SI Appendix*, Fig. S4*A*). Furthermore, hypoxia is expected to also directly affect the proliferation of the *Burkholderia* symbiont. Species of the genus *Burkholderia* are obligate aerobic bacteria, although they can tolerate microaerobic and anaerobic conditions (44–46). Accordingly, the *Burkholderia* symbiont grew normally in normoxia (21% O_2) but did not grow well in hypoxia (6 to 12% O_2) and anoxia (<0.1% O_2; *SI Appendix*, Fig. S4*B*). However, the bacteria incubated first in hypoxia or anoxia grew again when transferred to normoxia and cultured for an additional 48 h (*SI Appendix*, Fig. S4*B*), suggesting that *B. insecticola* needs enough oxygen for proliferation in vitro as well as in the midgut crypts. Furthermore, a *B. insecticola* mutant in the *resB* gene, essential for cytochrome *c* maturation and respiration, cannot properly colonize the M4 crypts (Fig. 4*C*). A reduced flux of oxygen and nutrients into the lumen of the crypts of *RpDuox*-RNAi insects could create a rapid depletion of these molecules, resulting in a gradient from the surface of the crypts toward their interior. Such an oxygen and/or nutrient gradient could explain the presence of a relatively high number of symbionts close to the epithelial surface of the midgut crypts and a lack of them in the interior part of the crypt lumen, as observed by TEM (Fig. 1*F*). Thus, the symbiosis defect in the *RpDuox*-RNAi insects is likely due to a lack of sufficient oxygen in the symbiotic organ that can sustain the respiratory activity of the symbiont.

Conversely, the high bacterial respiration in the M4 is the probable trigger of the extensive tracheal network in Sym insects. *B. insecticola* mutants in *fliC*, encoding the flagellin protein, and *uppP*, involved in cell wall synthesis, cannot colonize the M4 (7, 47), while a mutant in *purL*, involved in purine biosynthesis, can only weakly colonize the crypts (48) (Fig. 4*C*). The formation of tracheae was not, or less, stimulated in insects infected with these mutants (Fig. 4*C*), confirming that the mere presence of

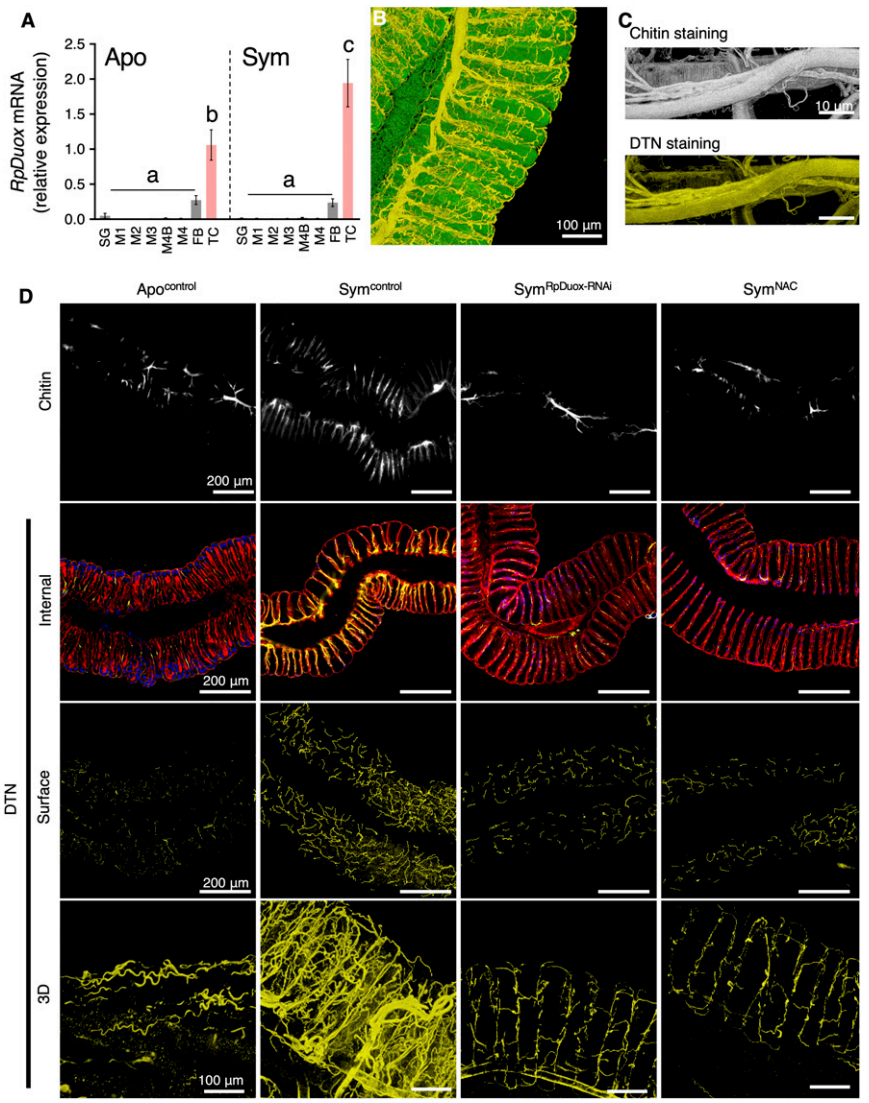

Fig. 3. Symbiont colonization triggers tracheal development, and RpDuox-mediated ROS stabilizes it by forming a DTN. (*A*) The relative expression of *RpDuox* in different tissues of Apo and Sym insects. Data shown are mean ± SD ($n = 4$ insects). Different letters indicate statistically significant differences ($P < 0.05$). The statistical significance of differences between samples was analyzed by a Kruskal–Wallis test with Bonferroni correction. (*B*) A 3D image of the tracheal network in the M4 of a $Sym^{control}$ insect. (*C*) Staining of the chitin and DTN of tracheae detached from the M4. (*D*) The tracheal network in the M4 of Apo ($Apo^{control}$), Sym ($Sym^{control}$), *RpDuox*-RNAi ($Sym^{RpDuox\text{-}RNAi}$), and NAC-fed (Sym^{NAC}) insects. The tracheal network, stained with Fluorescent Brightener 28 (calcofluor-white) to visualize chitin (first row), DTN in the internal section of the M4 (second row), DTN located on the surface of the M4 (third row), and 3D reconstitution of DTN of the tracheal network (fourth row). The colors in *B–D* are as follows: white, chitin; yellow, DTN; red, host cytoskeleton; blue, host nuclei; green, GFP signal derived from gut-colonizing symbionts.

Burkholderia in the midgut is not sufficient and that bacterial proliferation in the M4 crypts is required to trigger tracheal development.

Increased Oxygen Supply Compensates for the Lack of Tracheal Development and Restores Symbiosis in *RpDuox*-RNAi Insects. Next, we confirmed the crucial role of oxygen in gut symbiosis by rearing Sym and *RpDuox*-RNAi insects in hypoxia (6 to 12% O_2), normoxia (21% O_2), and hyperoxia (39 to 42% O_2) conditions (*SI Appendix*, Fig. S4*C*). The GFP signal of gut symbionts was diminished in Sym insects reared in a low-oxygen environment (Fig. 4*D*). In agreement with the microscopy observation, qPCR confirmed the decreased number of *Burkholderia* in the M4 crypts (*SI Appendix*, Fig. S4*D*). In contrast, when Sym insects were reared in hyperoxia, the number of gut-colonizing symbionts was not significantly increased, suggesting that the oxygen supply to maintain symbiosis is sufficient in normoxia (Fig. 4*D* and *SI Appendix*, Fig. S4*D*).

Contrary to Sym insects reared in normoxia, those reared in hyperoxia did not develop much of an enhanced tracheal network in the symbiotic organ compared to Apo insects (Fig. 4*E*). These results indicate that the available oxygen in the hyperoxia condition is sufficient to support symbiosis without the need for more tracheae and that the high oxygen consumption by symbiont colonization in the midgut is the trigger of the enhanced tracheal development in Sym insects in normoxia.

As described above, *RpDuox*-RNAi insects harbor only few symbiotic bacteria under normoxia, and, when they were reared in hypoxia, their symbiont titer was decreased even further (Fig. 4*D* and *SI Appendix*, Fig. S4*D*). However, the M4 crypt population of gut symbionts in *RpDuox*-RNAi insects considerably recovered in a hyperoxia environment (Fig. 4*D* and *SI*

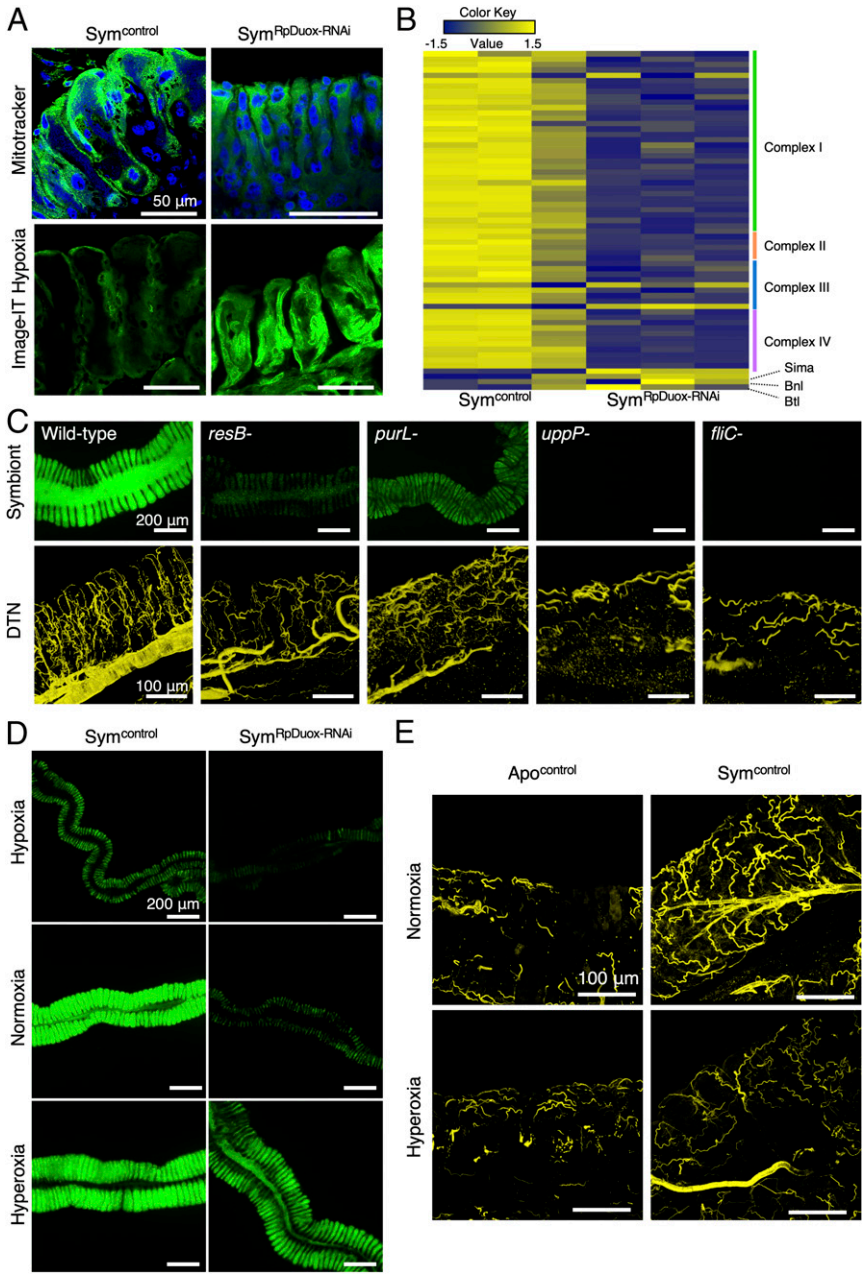

Fig. 4. Destabilization of the respiratory network by RpDuox-RNAi causes hypoxia in the midgut. (*A*) Active mitochondria in Sym ($Sym^{control}$) and *RpDuox*-RNAi ($Sym^{RpDuox\text{-}RNAi}$) insects stained by MitoTracker, a membrane potential fluorescence dye, which stains active mitochondria in live cells. Green, MitoTracker; blue, host nuclei (*Top*). Hypoxia in the M4 revealed by staining with Image-IT hypoxia fluorescence dye, a real-time oxygen detector (green; *Bottom*). (*B*) Heat map of relative expression levels of genes related to the host respiratory chain, *Sima*, *Branchless* (bnl), and *Breathless* (btl), in $Sym^{control}$ and $Sym^{RpDuox\text{-}RNAi}$ insects. Each column is a replicate experiment. (*C*) Colonization level of the wild type, *resB*-, *purL*-, *uppP*-, and *fliC*-deficient *B. insecticola* mutants in the symbiotic organ (*Top*). The DTN of the tracheal network from the symbiotic organs infected with wild type and *Burkholderia* mutants (*Lower*). Yellow color indicates the DTN signal of the tracheal network. (*D*) Observation by epifluorescence microscopy of the midgut of $Sym^{control}$ and $Sym^{RpDuox\text{-}RNAi}$ insects reared in hypoxia (6 to 12% O_2), normoxia (21% O_2), and hyperoxia (39 to 42% O_2) environments. Green is the GFP signal derived from *Burkholderia* gut symbionts. (*E*) Tracheal network in the M4 of $Apo^{control}$ and $Sym^{control}$ insects reared under normoxia and hyperoxia conditions.

Appendix, Fig. S4*D*). These results demonstrate that the availability of sufficient oxygen in the symbiotic organ is critical for a successful symbiosis and that a deficient oxygen supply is the major factor underpinning the symbiotic defect of *RpDuox*-RNAi insects.

Silencing of Regulators of Tracheal Development Simulates the Collapse of Symbiosis. To confirm the importance of oxygen distribution by the respiratory network in gut symbiosis, we silenced *branchless* (*RpBnl*) and *trachealess* (*RpTrh*), two known genes important for the tracheal development in *Drosophila* (49–51), as well as *RpSima*, encoding the hypoxia-inducible factor (HIF)-1α, which is a central regulator of the transcriptional response to hypoxia (52) and controls the expression of *Bnl* and *breathless* (*Btl*), another tracheal regulator (53). Thus, Sima, Trh, Bnl, and Btl constitute a regulatory module that controls tracheal development under low oxygen. The *RpTrh*-RNAi insects showed a high mortality (*SI Appendix*, Fig. S5*B*), but the alive insects and

those silenced for the other two genes had an underdeveloped respiratory network in the M4 (Fig. 5), in agreement with the expected role of *RpBnl* and *RpTrh* and further showing that oxygen-depletion signaling via Sima controls the tracheal development in the symbiotic organ. Crucially, the defect in the tracheal development in these RNAi insects is accompanied by a failure to establish the symbiosis with a full infection of the crypts, as revealed by the strongly decreased GFP signal derived from gut symbionts in the symbiotic organ (Fig. 5 and *SI Appendix*, Fig. S5*A*). Thus, the down-regulation of these three regulators of the respiratory system affected symbiosis in a very similar way as *RpDuox*-RNAi. The enhanced expression of *RpSima*, *RpBnl*, and *RpBtl* in the crypts of the *RpDuox*-RNAi insects (Fig. 4*B*) is in agreement with Sima still being active after *RpDuox* RNAi and thus with RpDuox acting downstream of the Sima/Btl/Trh/Bnl regulatory module.

Discussion

Our results demonstrate that the large population of the *Burkholderia* symbiont present in the body of the bean bug stimulates the sprouting of tracheal branches toward the symbiont-infected M4 crypts. We highlight a function of the Duox enzyme in this process, catalyzing the formation of a newly discovered tracheal DTN, which is essential for the stabilization of the respiratory network (Fig. 6). The tracheal system consists of a tubular epithelial network containing an extracellular luminal chitin and protein matrix (39, 40). Chitin is an essential component of this matrix, providing rigidity to the tracheal tubes, and mutants in chitin synthesis genes form misshapen tracheal tubes in *Drosophila* (41, 54). The matrix also contains proteins, including the zona pellucida domain proteins Piopio (Pio) and Dumpy (Dp), chitin-binding and remodeling proteins, and other unidentified protein components. They are thought to provide, together with the chitin scaffold, a structural network in the luminal space, regulating tube length, width, branching, and integrity (55–57). The requirement for Duox in the formation of new tracheae indicates that dityrosine cross-linking these matrix proteins is crucial for their structural function. Similar as in *R. pedestris*, we found that the expression of *Duox* is much higher in the tracheae than in the midgut in the phylogenetically diverse insects *Gryllus bimaculatus* (Orthoptera), *Bombyx mori* (Lepidoptera), *Tribolium castaneum* (Coleoptera), and *D. melanogaster* (Diptera; *SI Appendix*, Fig. S6). This conserved expression pattern suggests that the role of Duox in tracheae is common in the insects.

The pivotal role of Duox-mediated ROS in the formation of the tracheal cuticle proposed here adds to a number of other structures composed of extracellular matrices requiring Duox for DTN formation. These structures include the earlier-mentioned peritrophic matrix of the gut in the mosquito *A. gambiae* as well as in the tick *I. scapularis* (23, 24), the eggshell of the kissing bug (58), the cuticle structure of wings in *Drosophila* (59, 60), the collagenous extracellular cuticle matrix that forms the outer covering of nematodes (61), and the hardened extracellular matrix of sea urchin eggs after fertilization (62). Therefore, the importance of Duox in forming DTNs as part of the biogenesis of extracellular cuticle structures is conserved and not limited to insects. This function could be the ancestral and primary function of Duox enzymes.

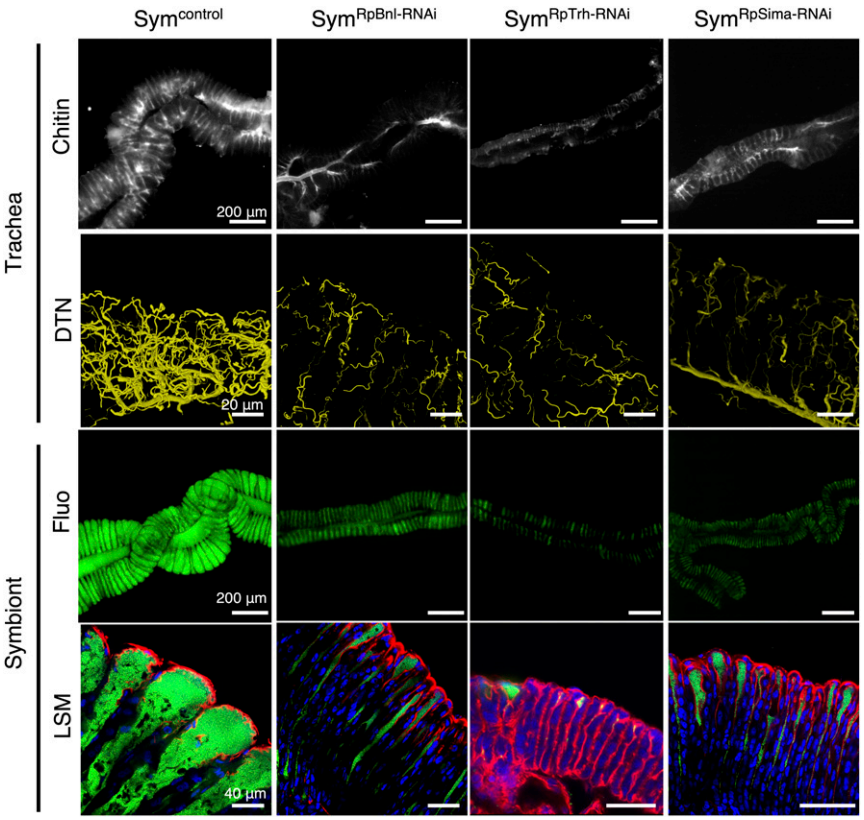

Fig. 5. Oxygen supply to the symbiotic organ via the tracheal network is important for gut symbiosis. Chitin staining (first row), 3D reconstruction of the DTN (second row), colonization by *Burkholderia* (third row), and crypt morphology (fourth row) in the M4 of Sym (Sym^{control}), *RpBnl*-RNAi (Sym$^{RpBnl\text{-}RNAi}$), *RpTrh*-RNAi (Sym$^{RpTrh\text{-}RNAi}$), and *RpSima*-RNAi (Sym$^{RpSima\text{-}RNAi}$) insects. Images were obtained by epifluorescence microscopy in the first and third rows and by laser scanning confocal microscopy in the second and fourth rows. White, chitin; yellow, DTN; green, gut symbiont; blue, host nuclei; red, host cytoskeleton.

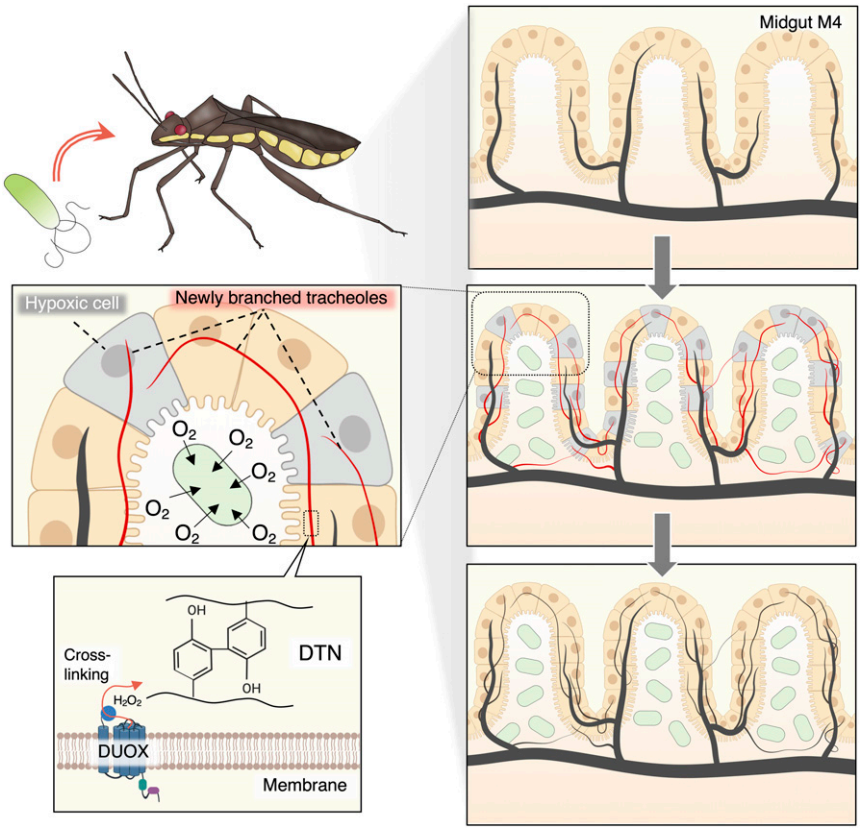

Fig. 6. RpDuox mediates symbiosis and tracheal network stability. Tracheal network in the M4 before symbiont infection (*Top Right*). Development of the tracheal network is stimulated to supply oxygen to the M4 when colonized by the symbiont, which consumes high levels of oxygen (*Middle Left and Right*; red, newly ramified tracheoles; green, gut symbiont; gray, epithelial cells experiencing reduced oxygen levels and attracting growing tracheoles). The branched tracheoles are stabilized by *RpDuox* (*Bottom Right*). RpDuox stabilizes the DTN of the tracheal cuticle layer, which is critical for structurally maintaining trachea (*Bottom Left*). The developmental order is in the direction of the arrows.

The formation of dityrosine cross-links in cuticle requires a NADPH oxidase to generate H_2O_2 and a heme peroxidase to catalyze the formation of a covalent bond between two neighboring tyrosine residues via tyrosyl radical formation and the reduction of H_2O_2. Potentially, both these functions are provided by Duox via its C-terminal NADPH oxidase domain and N-terminal peroxidase homology domain, respectively. In *Caenorhabditis elegans*, Duox is a self-contained catalyst that mediates tyrosine cross-linking independently (63). However, in mosquito, fly, and ticks, the peroxidase domain is only partially functional in DTN formation, and an additional secreted heme peroxidase protein is required for the formation of the dityrosine cross-links (23, 24, 59). The weak peroxidase activity of Duox in these organisms is believed to result from a mutation in a glutamic acid residue in the N-terminal peroxidase domain involved in heme binding (24). In the case of the *R. pedestris* RpDuox protein, the same point mutation is present, suggesting that the functionality of RpDuox may be similar to the tick, fly, and mosquito Duox enzymes. Therefore, we predict that the RpDuox enzyme works in concert with an additional, unidentified heme peroxidase to form the dityrosine bridges in the matrix proteins.

Often, the production of bactericidal ROS is presented as the principal function of Duox in insect physiology (14, 15, 22). In *Drosophila*, knockdown of *Duox* or *Mesh*, a positive regulator of *Duox* expression, leads to an increase of the gut microbiome load or to the persistence in the gut after oral infection of the entomopathogenic bacterium *Erwinia carotovora* ssp. *carotovora* strain *Ecc15* (20, 64). A similar role in direct killing of gut microbes was proposed in *C. elegans* (19). In striking contrast, we did not observe, after *Duox*-RNAi in the bean bug, an increase of the pathogen *S. marcescens* in the M3 digestive region of the midgut or of the symbiont in M3 or M4 crypts (Figs. 1*E* and 2 *B* and *C*). On the contrary, we noticed a strongly reduced symbiotic population in M4 (Fig. 1 *E* and *F*). In the mosquito *A. gambiae* and the tick *I. scapularis*, silencing *Duox* or the gene encoding the Duox partner peroxidase decreased the microbial load in the midgut rather than increasing it (23, 24). Together, these results indicate that the direct bactericidal activity of Duox as proposed originally in *Drosophila* is not universal in the insects and other arthropods. In light of this conclusion, we propose that the exclusive emphasis on the role of Duox in the production of antimicrobial ROS in the gut of *Drosophila* (14, 15, 22) should be revisited. It is likely that *Drosophila* Duox is also involved in the synthesis of the peritrophic matrix in the midgut and contributes through this activity as well to gut immunity. In agreement with this hypothesis, a mutation of the *Drosophila dcy* gene, encoding the drosocrystallin chitin-binding protein, results in a thinner but not completely abolished peritrophic matrix, which renders the flies more sensitive to gut infections with entomopathogenic bacteria (65, 66). This phenotype is reminiscent of the Duox RNAi flies, although the latter were more severely affected in immune response (12). Transglutaminase is another enzyme that affects protein–protein cross-linking and permeability in the peritrophic matrix of *Drosophila*, as well as the tolerance of the flies to the gut microbiota (67). Thus, Duox could have a dual contribution to the gut immune homeostasis in the case of *Drosophila*. On the contrary, the load of aerobic bacteria in the *Drosophila* midgut is much lower than in the *R. pedestris*

symbiotic organ (68). Therefore, Duox-mediated development of tracheae enveloping the midgut could possibly have a lesser importance for sustaining the microbiota or permitting pathogen development in *Drosophila*.

Nutritional cues via insulin-like and neuropeptide signaling give rise to changes in the tracheal architecture in the *Drosophila* midgut (69). Conversely, trachea-derived morphogens control midgut development by stimulating intestinal stem cells (70). Therefore, we can speculate that bacterial or host signals warning for enhanced nutritional requirements, are the triggers for the formation of the respiratory network enveloping the crypts, while, simultaneously, the growing tracheae produce morphogens that allow the swelling and opening of the crypts needed for bacterial colonization. On the other hand, hypoxia is the major known regulator of tracheal plasticity in *Drosophila* (53, 71). Therefore, low oxygen levels created by the metabolic activity of the proliferating symbionts and the crypt epithelial cells that nurture the symbiont could be the direct cause of tracheae genesis (Fig. 6). In agreement with the view of the symbiotic organ as an oxygen sink, we find no symbiosis-stimulated development of tracheae in insects reared in high oxygen levels (Fig. 4*E*) or when the insects were infected with symbiont mutants that have weak or no crypt colonization capacity (Fig. 4*C*). Moreover, Sima, Trh, and Bnl are required for tracheae development in a similar way as Duox. The *bnl* gene in *Drosophila* encodes a fibroblast growth factor homolog whose expression is highly increased in oxygen-starved nontracheal cells. Bnl exerts chemoattraction of tracheal cells via binding to the tracheae-specific receptor Btl that controls the ramification of tracheae toward the Bnl-producing cells (49, 71). The transcription factor Trh is a tracheal cell identity regulator, controlling tracheae-specific gene expression, including *btl* (50, 51). The HIF-1α homolog Sima in *Drosophila* is a central regulator of the transcriptional response to hypoxia. The Sima transcription factor is actively degraded in normoxia, dependent on the oxygen sensor Fatiga, but is stable and active in hypoxia (52, 72). Active Sima in hypoxia up-regulates the expression of *btl* in tracheal cells and *bnl* in nontracheal cells, thereby stimulating the development of the respiratory network (53). Thus, in *R. pedestris*, oxygen depletion in the symbiotic organ triggered by symbiont colonization is potentially enough as a signal to stabilize Sima in both the crypt epithelia and the local tracheal cells. Sima subsequently activates the transcription of, respectively, *RpBnl* and *RpBtl*, the latter also necessitating the tracheae-specific transcription factor Trh. This signaling cascade controls the expression of the genes required for the development of the tracheal network around the crypts, which most likely also includes *RpDuox*. Thus, *RpDuox* gene expression and protein activity, being an inherent part of tracheal development, is indirectly induced by the establishment of the symbiosis via the enhanced trachea formation.

In a remarkable analogous process to the tracheal development in the colonized midgut of *R. pedestris*, colonization of the mammalian small intestine by microbiota promotes angiogenesis and the development of the blood vessel network around the gut epithelia. This enhanced vascularization increases oxygenation of the villi, which have a modified morphology after colonization and an increased nutrient absorption activity (73–75). Thus, from insects to mammals, colonization of the gut by symbionts can create a local oxygen sink, triggering an analogous postembryonic developmental response.

Besides the midgut crypts of *R. pedestris* and related stinkbugs, other types of symbiotic organs in other insects, such as bacteriomes (9, 76), are equally enveloped by a tracheal network, presumably to provide oxygen to the respiring symbiotic bacteria (77, 78). These symbioses might therefore depend on Duox activity as well. Feeding *Drosophila* and *C. elegans* with different types of antioxidant chemicals inhibits Duox-produced ROS (19, 64). Here, we show that feeding *R. pedestris* with the antioxidant NAC is sufficient to prevent the accumulation of ROS produced by Duox and the sprouting of the tracheae, and this blocks the establishment of symbiosis. Since many insects obligatorily depend on their symbioses, triggering their collapse by the specific inhibition of the respiratory network with antioxidants could be a new route to fight insect pests.

Materials and Methods

Insect Rearing and Infection with Symbiont. The *R. pedestris* strain used in this study was originally collected from a soybean field in Tsukuba, Ibaraki, Japan, and maintained in the laboratory for over 10 y. The bean bugs were reared in Petri dishes (90 mm in diameter and 20 mm high) under a long-day regimen (16 h light and 8 h dark) at 25 °C and fed with soybean seeds and distilled water containing 0.05% ascorbic acid (DWA). To infect insects with symbionts, *B. insecticola* (RPE75), GFP-expressing *B. insecticola* (RPE225), or mutant *Burkholderia* strains (*SI Appendix*, Table S1) were orally administered to second-instar nymphs by supplying the bacteria at a density of 10^7 cells per milliliter to the DWA. To feed NAC, DWA with 10 mg/mL of NAC was supplied to the bean bugs. *T. castaneum* was a gift of Ryo Futahashi (National Institute of Advanced Industrial Science and Technology Tsukuba Center, Tsukuba, Japan). *G. bimaculatus* and *B. mori* were purchased from a pet shop in Sapporo, Japan.

Detection of ROS Levels. Fourth-instar nymphs of bean bugs were dissected in phosphate-buffered saline (PBS), pH 7.4, using fine forceps under a dissection microscope (S8APO and MZ FZ III; Leica), and each part of their midguts was transferred to 1.5-mL microcentrifuge tubes and homogenized by a pestle. The homogenized midgut samples were centrifuged at 15,000 rpm for 1 min to remove tissue debris, and the supernatant was transferred to the 96-well black polystyrene microplate and incubated with 50 μM 2′,7′-dichlorofluorescein diacetate (Thermo Fisher Scientific) for 20 min in the dark. The ROS level in each sample was measured by a microplate reader (Infinite F200 PRO; Tecan) using an excitation wavelength of 488 nm and an emission wavelength of 535 nm.

Synthesis of Double-Stranded RNA and RNAi. Gene sequences of *Duox*, *RpRelish*, *RpTrh*, *RpBnl*, and *RpSima* were identified by an RNA-sequencing analysis of symbiotic insects and BLAST identification using the *Drosophila* proteins as search term (accession nos. MT270146–MT270150). Fragments of target genes for RNAi knockdown were obtained from *R. pedestris* cDNA. The fifth-instar nymphs of bean bugs were dissected in PBS, and total RNA was extracted from the M4 using RNAiso Plus (Takara Bio) and the RNeasy Mini Kit (Qiagen). The cDNA was synthesized from 1 μg of extracted total RNA by PrimeScript RT Reagent Kit with gDNA Erase (Takara Bio).

To synthesize dsRNA for RNAi, ∼500-bp fragments of the target gene were amplified from cDNA, with primers listed in *SI Appendix*, Table S2. The PCR products were cloned in the pT7Blue T-vector and transformed into *Escherichia coli* DH5α cells. Clones were verified by sequencing. Next, the target gene was amplified by PCR from these plasmids using specific upstream and downstream primers, each extended with the T7 promotor sequences (*SI Appendix*, Table S2), to create a template for RNA polymerization. The dsRNA was synthesized from these PCR products by the MEGAscript RNAi kit (Thermo Fisher Scientific).

To silence a target gene, 100 ng of the corresponding dsRNA was injected into the hemolymph between the torso and hind leg of the symbiont-infected second-instar nymph of bean bugs after 2 d of symbiont infection using a glass capillary and a FemtoJet microinjector (Eppendorf). For triggering a septic injury, 10^7 *E. coli* DH5α cells were similarly injected in the hemolymph. The phenotypic alteration in the insects was observed 1 wk after RNAi. The detailed timeline of the experiment is described in *SI Appendix*, Fig. S7.

Estimation of Infection Levels of Symbiotic Organs by qPCR. To measure the number of symbionts present in the M4, DNA was extracted from the dissected M4 by the QIAamp DNA Mini Kit (Qiagen), and real-time qPCR was performed using primers BSdnaA-F and BSdnaA-R (*SI Appendix*, Table S2), which target the *dnaA* gene of the *Burkholderia* symbiont, the KAPA SYBR FAST qPCR Master Mix Kit (KAPA Biosystems), and the Roche LightCycler 96 System (Roche). The number of gut symbionts was calculated based on a standard curve for the *dnaA* gene containing 10, 10^2, 10^3, 10^4, 10^5, 10^6, and 10^7 copies per reaction of the target PCR product.

Gene Expression Determination by RT-qPCR. To measure the mRNA expression level of the target genes, total RNA was extracted from the salivary gland, the midgut regions, the fat body, or the tracheae of the Apo and Sym bean bugs

and reverse-transcribed to cDNA as described above. The real-time qPCR for target genes was performed as described above using primers listed in *SI Appendix*, Table S2. The efficiency of the RNAi process on target genes and change of gene-expression patterns of immune genes was measured 3 d after RNAi (*SI Appendix*, Fig. S7). The mRNA levels were normalized by the elongation factor 1-alpha (EF1α) housekeeping gene.

Microscopy Analyses. To analyze the infection level of control, RNAi, or NAC-treated insects, the bean bugs were infected with GFP-expressing *Burkholderia* symbionts and injected with dsRNA or fed with NAC (*SI Appendix*, Fig. S7). After 1 wk, the M4 organs of fourth-instar bean bugs were dissected in PBS, transferred to a glass-bottom dish (Matsunami), and covered with a cover glass. The GFP signal derived from the M4-colonizing gut symbionts was observed with an epifluorescence microscope (DMI4000B; Leica).

Alternatively, to observe the colonization of the M4 by the gut symbiont with confocal microscopy, the bean bugs harboring GFP-expressing symbionts were dissected in PBS and the midgut was transferred to a 2-mL microcentrifuge tube. The gut samples were fixed with 4% paraformaldehyde (pH 7.4) for 10 min at 25 °C. The fixed samples were washed three times by PBS and permeabilized by PBS with 0.1% Triton X-100 (PBST) for 10 min at 25 °C. After permeabilization, the gut samples were washed again three times by PBS and stained with 4′6-diamidino-2-phenylindole (DAPI) and Alexa Fluor 647 Phalloidin for 30 min at 25 °C to stain, respectively, the nucleus and cytoskeleton of host cells. Then, the samples were transferred to a glass-bottom dish, mounted with ProLong Gold Antifade Mountant (Thermo Fisher Scientific), and observed under a laser scanning confocal microscope (TCS SP8; Leica).

Dityrosine networks were revealed by immunostaining. The whole gut of the fourth instar of control or RNAi bean bugs was dissected in PBS and fixed with 4% paraformaldehyde. The fixed midgut was permeabilized and incubated with blocking buffer (1% BSA in PBST) for 30 min at 25 °C. Then, the gut was stained with 1:400 dilution of anti-dityrosine monoclonal antibody (MyBioScience) overnight at 4 °C. Subsequently, the midgut was washed three times by PBS, each for 10 min, and then stained with 1:500 dilution of goat anti-mouse immunoglobulin G heavy and light chains conjugated with Alexa Fluor 555 (Abcam) for 1 h at 25 °C in the dark. The midgut was washed three times by PBS, each for 10 min, and then incubated with DAPI and phalloidin. The midgut was transferred to a glass-bottom dish, mounted, and observed with a laser scanning confocal microscope. The three-dimensional (3D) image of the DTN was reconstructed from *z*-stacked images using Leica LAS X software.

To observe the tracheal network by chitin fluorescent labeling, dissected midguts were stained with the Fluorescent Brightener 28 (Sigma-Aldrich) at a final concentration of 0.1 mg/mL for 5 min in the dark. Then, the midgut was washed three times by PBS, transferred to a glass-bottom dish, and observed with a confocal or epifluorescence microscope.

To analyze the hypoxic condition of the midgut, dissected M4 was stained with 10 μM Image-iT Green Hypoxia Reagent (Invitrogen) for 30 min at 25 °C and observed with a confocal microscope. To label active mitochondria, dissected midguts were incubated with 100 nM MitoTracker Green FM (Invitrogen) for 30 min at 25 °C and observed with a confocal microscope.

For TEM observations, the bean bugs were dissected with fine forceps in fixative solution (0.1 M sodium phosphate buffer containing 2.5% glutaraldehyde, pH 7.4). The isolated M4 was prefixed in the fixative solution at 4 °C overnight and postfixed in 2% osmium tetroxide at 4 °C for 1 h. After a series of dehydration steps by ethanol, the gut was embedded in Epon812 resin (TAAB). Ultrathin sections were made by using an ultramicrotome (EM UC7; Leica), mounted on a copper mesh, stained with uranyl acetate and lead citrate, and observed under a transmission electron microscope (H-7600; Hitachi).

Colony-Forming Unit Assay. Cultured *S. marcescens* (10^7 cells per milliliter) were orally administrated to the third instar of Sym and *RpDuox*-RNAi bean bugs. The midgut M3 regions were dissected 3 d after infection and homogenized with a pestle in 100 μL of PBS. After the serial dilution of these M3 lysates, 10 μL of the dilutions was spotted on a Luria broth agar plate with 30 μg/mL of rifampicin, and plates were incubated at 30 °C for 1 d to obtain bacterial growth. To measure the symbiont titer in the M3 of Sym and *RpDuox*-RNAi bean bugs, dsRNA of *RpDuox* was injected to second-instar nymphs of Apo insects, and then newly molted third-instar nymphs were infected with cultured *Burkholderia* symbionts (10^7 cells per milliliter) and the M3 was dissected 24 h after infection. The dissected M3 was homogenized, and dilution series were spotted on a yeast glucose (YG) agar plate with 30 μg/mL of rifampicin, which was incubated for 2 d at 30 °C.

Bacterial Growth and Insect Rearing in Hypoxia and Hyperoxia Conditions. To culture the *Burkholderia* symbiont in anaerobic or microaerophilic conditions, agar plates were placed in a 2.5-L W-zip standing pouch jar (Mitsubishi Gas Chemical) containing, respectively, an Anaero Pack-Anaero (O_2 <0.1%) or an Anaero Pack-MicroAero (6% < O_2 < 12%; Mitsubishi Gas Chemical). Plates were incubated for 48 h at 30 °C and subsequently for a further 48 h at 30 °C in normoxia condition.

To rear insects in a hypoxia environment, Petri dishes containing second-instar nymphs were placed in a 2.5-L rectangular jar containing an Anaero Pack-MicroAero. To create the hyperoxia condition, Petri dishes containing second-instar nymphs were placed in a culture jar, and oxygen was injected daily via a valve in order to maintain 39 to 42% oxygen as shown in *SI Appendix*, Fig. S4*C*. The oxygen content (as a percentage) in the jar was monitored by an oxygen indicator (OXY-M; JICKO). Additional methods are described in *SI Appendix*, *Supplementary Text*.

Data Availability. RNA-seq data of the M4 of Symcontrol and SymRpDuox-RNAi; gene sequences of RpDuox, RpBnl, RpTrh, RpSima, and RpRelish; and sequences of Duox of *G. bimaculatus*, *B. mori*, and *T. castaneum* data have been deposited in the National Center for Biotechnology Information (BioProject PRJDB9456) GenBank database (DRA accession numbers DRR215696-DRR215701; MT270146-MT270150; MT270151, NW_004582026, and NC_007418).

ACKNOWLEDGMENTS. We thank H. Ooi (National Institute of Advanced Industrial Science and Technology [AIST]) for insect rearing; X.-Y. Meng and M. Kanno (AIST) for help with electron microscopy; and Y. Matsuura (The University of the Ryukyus), K. Takeshita (Akita Prefecture University), and S. Kanie (AIST) for critical comments on the manuscript. This study was supported by Japan Society for the Promotion of Science (JSPS) Research Fellowships for Young Scientists to S.J. (201911493) and T.O. (20170267 and 19J01106); by Ministry of Education, Culture, Sports, Science and Technology KAKENHI to Y.K. (18KK0211 and 20H03303); and by a JSPS-CNRS Bilateral Open Partnership Joint Research Project and the CNRS International Research Project "Ménage à Trois" to Y.K. and P.M.

1. N. A. Moran, H. Ochman, T. J. Hammer, Evolutionary and ecological consequences of gut microbial communities. *Annu. Rev. Ecol. Evol. Syst.* **50**, 451–475 (2019).
2. R. E. Ley *et al*., Evolution of mammals and their gut microbes. *Science* **320**, 1647–1651 (2008).
3. A. E. Douglas, Multiorganismal insects: Diversity and function of resident microorganisms. *Annu. Rev. Entomol.* **60**, 17–34 (2015).
4. H. Itoh, K. Tago, M. Hayatsu, Y. Kikuchi, Detoxifying symbiosis: Microbe-mediated detoxification of phytotoxins and pesticides in insects. *Nat. Prod. Rep.* **35**, 434–454 (2018).
5. H. Vogel *et al*., The digestive and defensive basis of carcass utilization by the burying beetle and its microbiota. *Nat. Commun.* **8**, 15186 (2017).
6. R. J. Dillon, V. M. Dillon, The gut bacteria of insects: Nonpathogenic interactions. *Annu. Rev. Entomol.* **49**, 71–92 (2004).
7. T. Ohbayashi *et al*., Insect's intestinal organ for symbiont sorting. *Proc. Natl. Acad. Sci. U.S.A.* **112**, E5179–E5188 (2015).
8. M. C. Lanan, P. A. P. Rodrigues, A. Agellon, P. Jansma, D. E. Wheeler, A bacterial filter protects and structures the gut microbiome of an insect. *ISME J.* **10**, 1866–1876 (2016).
9. P. Buchner, *Endosymbiosis of Animals with Plant Microorganisms* (Interscience Publishers, New York, 1965).
10. S. Jang, Y. Kikuchi, Impact of the insect gut microbiota on ecology, evolution, and industry. *Curr. Opin. Insect Sci.* **41**, 33–39 (2020).
11. J. H. Yun *et al*., Insect gut bacterial diversity determined by environmental habitat, diet, developmental stage, and phylogeny of host. *Appl. Environ. Microbiol.* **80**, 5254–5264 (2014).
12. E. M. Ha, C. T. Oh, Y. S. Bae, W. J. Lee, A direct role for dual oxidase in *Drosophila* gut immunity. *Science* **310**, 847–850 (2005).
13. K. A. Lee *et al*., Bacterial-derived uracil as a modulator of mucosal immunity and gut-microbe homeostasis in *Drosophila*. *Cell* **153**, 797–811 (2013).
14. N. Buchon, N. Silverman, S. Cherry, Immunity in *Drosophila melanogaster*–From microbial recognition to whole-organism physiology. *Nat. Rev. Immunol.* **14**, 796–810 (2014).
15. T. Kuraishi, A. Hori, S. Kurata, Host-microbe interactions in the gut of *Drosophila melanogaster*. *Front. Physiol.* **4**, 375 (2013).
16. E. M. Ha *et al*., Coordination of multiple dual oxidase-regulatory pathways in responses to commensal and infectious microbes in *drosophila* gut. *Nat. Immunol.* **10**, 949–957 (2009).
17. E. M. Ha *et al*., Regulation of DUOX by the Galphaq-phospholipase Cbeta-Ca2+ pathway in Drosophila gut immunity. *Dev. Cell* **16**, 386–397 (2009).
18. Y. S. Bae, M. K. Choi, W. J. Lee, Dual oxidase in mucosal immunity and host-microbe homeostasis. *Trends Immunol.* **31**, 278–287 (2010).
19. V. Chávez, A. Mohri-Shiomi, D. A. Garsin, Ce-Duox1/BLI-3 generates reactive oxygen species as a protective innate immune mechanism in *Caenorhabditis elegans*. *Infect. Immun.* **77**, 4983–4989 (2009).

20. X. Xiao *et al*., A Mesh-Duox pathway regulates homeostasis in the insect gut. *Nat. Microbiol.* **2**, 17020 (2017).
21. J. H. Ryu *et al*., An essential complementary role of NF-kappaB pathway to microbicidal oxidants in Drosophila gut immunity. *EMBO J.* **25**, 3693–3701 (2006).
22. S. H. Kim, W. J. Lee, Role of DUOX in gut inflammation: Lessons from *Drosophila* model of gut-microbiota interactions. *Front. Cell. Infect. Microbiol.* **3**, 116 (2014).
23. S. Kumar, A. Molina-Cruz, L. Gupta, J. Rodrigues, C. Barillas-Mury, A peroxidase/dual oxidase system modulates midgut epithelial immunity in *Anopheles gambiae*. *Science* **327**, 1644–1648 (2010).
24. X. Yang, A. A. Smith, M. S. Williams, U. Pal, A dityrosine network mediated by dual oxidase and peroxidase influences the persistence of Lyme disease pathogens within the vector. *J. Biol. Chem.* **289**, 12813–12822 (2014).
25. T. Ohbayashi, P. Mergaert, Y. Kikuchi, Host-symbiont specificity in insects: Underpinning mechanisms and evolution. *Adv. Insect Phys.* 58, 27–62 (2020).
26. K. Takeshita, Y. Kikuchi, *Riptortus pedestris* and *Burkholderia* symbiont: An ideal model system for insect-microbe symbiotic associations. *Res. Microbiol.* **168**, 175–187 (2017).
27. M. Kaltenpoth, L. V. Flórez, Versatile and dynamic symbioses between insects and *Burkholderia* bacteria. *Annu. Rev. Entomol.* **65**, 145–170 (2020).
28. T. Ohbayashi *et al*., Comparative cytology, physiology and transcriptomics of *Burkholderia insecticola* in symbiosis with the bean bug *Riptortus pedestris* and in culture. *ISME J.* **13**, 1469–1483 (2019).
29. H. Itoh *et al*., Host-symbiont specificity determined by microbe-microbe competition in an insect gut. *Proc. Natl. Acad. Sci. U.S.A.* **116**, 22673–22682 (2019).
30. Y. Kikuchi, T. Ohbayashi, S. Jang, P. Mergaert, *Burkholderia* insecticola triggers midgut closure in the bean bug *Riptortus pedestris* to prevent secondary bacterial infections of midgut crypts. *ISME J.* **14**, 1627–1638 (2020).
31. R. Futahashi *et al*., Gene expression in gut symbiotic organ of stinkbug affected by extracellular bacterial symbiont. *PLoS One* **8**, e64557 (2013).
32. P. Mergaert, Y. Kikuchi, S. Shigenobu, E. C. M. Nowack, Metabolic integration of bacterial endosymbionts through antimicrobial peptides. *Trends Microbiol.* **25**, 703–712 (2017).
33. K. E. Park *et al*., The roles of antimicrobial peptide, rip-thanatin, in the midgut of *Riptortus pedestris*. *Dev. Comp. Immunol.* **78**, 83–90 (2018).
34. Y. Kikuchi, X.-Y. Meng, T. Fukatsu, Gut symbiotic bacteria of the genus *Burkholderia* in the broad-headed bugs *Riptortus clavatus* and *Leptocorisa chinensis* (Heteroptera: Alydidae). *Appl. Environ. Microbiol.* **71**, 4035–4043 (2005).
35. O. I. Aruoma, B. Halliwell, B. M. Hoey, J. Butler, The antioxidant action of N-acetylcysteine: Its reaction with hydrogen peroxide, hydroxyl radical, superoxide, and hypochlorous acid. *Free Radic. Biol. Med.* **6**, 593–597 (1989).
36. A. J. P. Goodchild, Studies on the fucntional anatomy of the intestines of heteroptera. *J. Zool.* **141**, 851–910 (1963).
37. J. K. Kim *et al*., Insect gut symbiont susceptibility to host antimicrobial peptides caused by alteration of the bacterial cell envelope. *J. Biol. Chem.* **290**, 21042–21053 (2015).
38. Y. Nishide *et al*., Functional crosstalk across IMD and Toll pathways: Insight into the evolution of incomplete immune cascades. *Proc. Biol. Sci.* **286**, 20182207 (2019).
39. S. Hayashi, T. Kondo, Development and function of the *Drosophila* tracheal system. *Genetics* **209**, 367–380 (2018).
40. J. Schottenfeld, Y. Song, A. S. Ghabrial, Tube continued: Morphogenesis of the *Drosophila* tracheal system. *Curr. Opin. Cell Biol.* **22**, 633–639 (2010).
41. W. P. Devine *et al*., Requirement for chitin biosynthesis in epithelial tube morphogenesis. *Proc. Natl. Acad. Sci. U.S.A.* **102**, 17014–17019 (2005).
42. D. Bandarra, J. Biddlestone, S. Mudie, H. A. Muller, S. Rocha, Hypoxia activates IKK-NF-κB and the immune response in *Drosophila melanogaster*. *Biosci. Rep.* **34**, e00127 (2014).
43. D. Zhou *et al*., Mechanisms underlying hypoxia tolerance in *Drosophila melanogaster*: Hairy as a metabolic switch. *PLoS Genet.* **4**, e1000221 (2008).
44. M. A. Hamad *et al*., Adaptation and antibiotic tolerance of anaerobic *Burkholderia pseudomallei*. *Antimicrob. Agents Chemother.* **55**, 3313–3323 (2011).
45. A. M. Sass *et al*., The unexpected discovery of a novel low-oxygen-activated locus for the anoxic persistence of *Burkholderia cenocepacia*. *ISME J.* **7**, 1568–1581 (2013).
46. G. Pessi *et al*., Response of *Burkholderia cenocepacia* H111 to micro-oxia. *PLoS One* **8**, e72939 (2013).
47. J. K. Kim *et al*., Bacterial cell wall synthesis gene *uppP* is required for *Burkholderia* colonization of the Stinkbug Gut. *Appl. Environ. Microbiol.* **79**, 4879–4886 (2013).
48. J. K. Kim *et al*., Purine biosynthesis-deficient *Burkholderia* mutants are incapable of symbiotic accommodation in the stinkbug. *ISME J.* **8**, 552–563 (2014).
49. D. Sutherland, C. Samakovlis, M. A. Krasnow, Branchless encodes a *Drosophila* FGF homolog that controls tracheal cell migration and the pattern of branching. *Cell* **87**, 1091–1101 (1996).
50. S. Chung, C. Chavez, D. J. Andrew, Trachealess (Trh) regulates all tracheal genes during *Drosophila* embryogenesis. *Dev. Biol.* **360**, 160–172 (2011).
51. R. Wilk, I. Weizman, B. Z. Shilo, Trachealess encodes a bHLH-PAS protein that is an inducer of tracheal cell fates in *Drosophila*. *Genes Dev.* **10**, 93–102 (1996).
52. S. Lavista-Llanos *et al*., Control of the hypoxic response in *Drosophila melanogaster* by the basic helix-loop-helix PAS protein similar. *Mol. Cell. Biol.* **22**, 6842–6853 (2002).
53. L. Centanin *et al*., Cell autonomy of HIF effects in *Drosophila*: Tracheal cells sense hypoxia and induce terminal branch sprouting. *Dev. Cell* **14**, 547–558 (2008).
54. A. Tonning *et al*., A transient luminal chitinous matrix is required to model epithelial tube diameter in the *Drosophila* trachea. *Dev. Cell* **9**, 423–430 (2005).
55. S. Luschnig, T. Bätz, K. Armbruster, M. A. Krasnow, Serpentine and vermiform encode matrix proteins with chitin binding and deacetylation domains that limit tracheal tube length in *Drosophila*. *Curr. Biol.* **16**, 186–194 (2006).
56. S. Wang *et al*., Septate-junction-dependent luminal deposition of chitin deacetylases restricts tube elongation in the *Drosophila* trachea. *Curr. Biol.* **16**, 180–185 (2006).
57. A. Jaźwińska, C. Ribeiro, M. Affolter, Epithelial tube morphogenesis during *Drosophila* tracheal development requires Piopio, a luminal ZP protein. *Nat. Cell Biol.* **5**, 895–901 (2003).
58. F. A. Dias *et al*., Ovarian dual oxidase (Duox) activity is essential for insect eggshell hardening and waterproofing. *J. Biol. Chem.* **288**, 35058–35067 (2013).
59. T. R. Hurd, F. X. Liang, R. Lehmann, Curly encodes dual oxidase, which acts with heme peroxidase curly Su to shape the adult *Drosophila* wing. *PLoS Genet.* **11**, e1005625 (2015).
60. N. T. T. Anh, M. Nishitani, S. Harada, M. Yamaguchi, K. Kamei, Essential role of Duox in stabilization of *Drosophila* wing. *J. Biol. Chem.* **286**, 33244–33251 (2011).
61. W. A. Edens *et al*., Tyrosine cross-linking of extracellular matrix is catalyzed by Duox, a multidomain oxidase/peroxidase with homology to the phagocyte oxidase subunit gp91phox. *J. Cell Biol.* **154**, 879–891 (2001).
62. J. L. Wong, G. M. Wessel, Extracellular matrix modifications at fertilization: Regulation of dityrosine crosslinking by transamidation. *Development* **136**, 1835–1847 (2009).
63. J. L. Meitzler, R. Brandman, P. R. Ortiz de Montellano, Perturbed heme binding is responsible for the blistering phenotype associated with mutations in the *Caenorhabditis elegans* dual oxidase 1 (DUOX1) peroxidase domain. *J. Biol. Chem.* **285**, 40991–41000 (2010).
64. E. M. Ha *et al*., An antioxidant system required for host protection against gut infection in *Drosophila*. *Dev. Cell* **8**, 125–132 (2005).
65. T. Kuraishi, O. Binggeli, O. Opota, N. Buchon, B. Lemaitre, Genetic evidence for a protective role of the peritrophic matrix against intestinal bacterial infection in *Drosophila melanogaster*. *Proc. Natl. Acad. Sci. U.S.A.* **108**, 15966–15971 (2011).
66. A. Hori, S. Kurata, T. Kuraishi, Unexpected role of the IMD pathway in *Drosophila* gut defense against *Staphylococcus aureus*. *Biochem. Biophys. Res. Commun.* **495**, 395–400 (2018).
67. T. Shibata *et al*., Transglutaminase-catalyzed protein-protein cross-linking suppresses the activity of the NF-κB-like transcription factor relish. *Sci. Signal.* **6**, ra61 (2013).
68. C. Ren, P. Webster, S. E. Finkel, J. Tower, Increased internal and external bacterial load during *Drosophila* aging without life-span trade-off. *Cell Metab.* **6**, 144–152 (2007).
69. G. A. Linneweber *et al*., Neuronal control of metabolism through nutrient-dependent modulation of tracheal branching. *Cell* **156**, 69–83 (2014).
70. Z. Li, Y. Zhang, L. Han, L. Shi, X. Lin, Trachea-derived dpp controls adult midgut homeostasis in *Drosophila*. *Dev. Cell* **24**, 133–143 (2013).
71. J. Jarecki, E. Johnson, M. A. Krasnow, Oxygen regulation of airway branching in *Drosophila* is mediated by branchless FGF. *Cell* **99**, 211–220 (1999).
72. R. K. Bruick, S. L. McKnight, A conserved family of prolyl-4-hydroxylases that modify HIF. *Science* **294**, 1337–1340 (2001).
73. F. Sommer, F. Bäckhed, The gut microbiota–Masters of host development and physiology. *Nat. Rev. Microbiol.* **11**, 227–238 (2013).
74. C. Reinhardt *et al*., Tissue factor and PAR1 promote microbiota-induced intestinal vascular remodelling. *Nature* **483**, 627–631 (2012).
75. T. S. Stappenbeck, L. V. Hooper, J. I. Gordon, Developmental regulation of intestinal angiogenesis by indigenous microbes via Paneth cells. *Proc. Natl. Acad. Sci. U.S.A.* **99**, 15451–15455 (2002).
76. P. Baumann, Biology bacteriocyte-associated endosymbionts of plant sap-sucking insects. *Annu. Rev. Microbiol.* **59**, 155–189 (2005).
77. P. Łukasik *et al*., Multiple origins of interdependent endosymbiotic complexes in a genus of cicadas. *Proc. Natl. Acad. Sci. U.S.A.* **115**, E226–E235 (2018).
78. B. Weiss, M. Kaltenpoth, Bacteriome-localized intracellular symbionts in pollen-feeding beetles of the genus Dasytes (Coleoptera, Dasytidae). *Front. Microbiol.* **7**, 1486 (2016).